# Getting to the Root of Plant-Mediated Methane Emissions and Oxidation in a Thermokarst Bog

**Jesse C. Turner[1*], Colby J. Moorberg[1†], Andrea Wong[1], Kathleen Shea[2‡], Mark P. Waldrop[3], Merritt R. Turetsky[2], Rebecca B. Neumann[1]**

[1]Department of Civil and Environmental Engineering, University of Washington, Seattle, WA USA.

[2]Department of Integrative Biology, University of Guelph, Ontario, Canada.

[3]U.S. Geological Survey, Menlo Park, CA USA.

Corresponding author: Rebecca B. Neumann (rbneum@uw.edu)

*Current address: SMRU Consulting, Friday Harbor, WA USA

†Current address: Department of Agronomy, Kansas State University, Manhattan, KS USA

‡Current address: Mackenzie Valley Environmental Impact Review Board, Yellowknife NT Canada

**Key Points:**

- In the presence of vascular vegetation, methane production increased and methane oxidation decreased, leading to greater methane emissions
- Minimal methane oxidation occurred along the plant-transport pathway, and methane oxidation was suppressed outside the plant pathway
- Data imply plants decreased oxidation by causing competition between methanotrophs and other heterotrophs for electron acceptors

## Abstract

Vascular plants are important in the wetland methane cycle but their effect on production, oxidation, and transport has high uncertainty, limiting our ability to predict emissions. In a permafrost-thaw bog in Interior Alaska, we used plant manipulation treatments, field-deployed planar optical oxygen sensors, direct measurements of methane oxidation, and microbial DNA analyses to disentangle mechanisms by which vascular vegetation affect methane emissions. Vegetation operated on top of baseline methane emissions, which varied with proximity to the thawing permafrost margin. Emissions from vegetated plots increased over the season, resulting in cumulative seasonal methane emissions that were 4.1–5.2 g $m^{-2}$ $season^{-1}$ greater than unvegetated plots. Mass balance calculations signify these greater emissions were due to increased methane production (3.0–3.5 g $m^{-2}$ $season^{-1}$) and decreased methane oxidation (1.1–1.6 g $m^{-2}$ $season^{-1}$). Minimal oxidation occurred along the plant-transport pathway and oxidation was suppressed outside the plant pathway. Our data indicate suppression of methane oxidation was stimulated by root exudates fueling competition among microbes for electron acceptors. This contention is supported by the fact that methane oxidation and relative abundance of methanotrophs decreased over the season in the presence of vegetation, but methane oxidation remained steady in unvegetated treatments; oxygen was not detected around plant roots, but was detected around silicone tubes mimicking aerenchyma; and oxygen injection experiments suggested that oxygen consumption was faster in the presence of vascular vegetation. Root exudates are known to fuel methane production and our work provides evidence they also decrease methane oxidation.



## Plain Language Summary

Methane is a greenhouse gas with a greater ability to warm the earth than carbon dioxide. Wetlands are the largest natural source of methane to the atmosphere. To understand future climate change, scientists need to predict the amount of methane released from wetlands. Many factors affect the amount of methane generated by soil microbes (called methane production) and how much methane is released into the atmosphere (called methane emission). Methane traveling through soils can also get converted to carbon dioxide through methane oxidation. Wetland plants influence production, transport and oxidation of methane, but studies disagree on their overall effect on emission. In this study, we used multiple methods to identify how plants affect the methane cycle. Plants appeared to increase methane production and, to our surprise, decrease methane oxidation. We created a theory for why plants increased methane emissions, advancing understanding of plant-soil interactions that contribute to wetland methane emissions.

## 1 Introduction

Wetlands represent the largest natural source of atmospheric methane ($CH_4$), contributing 20-40% of global emissions (Ciasis et al., 2013). Modeling of wetland-methane feedbacks indicates that wetland methane emissions could drive 21st century climate change, with global wetland emissions matching or exceeding anthropogenic emissions by 2100 (Zhang et al., 2017). However, modeled $CH_4$ emissions have high variability (Ciais et al., 2013; Melton et al., 2013), partly due to poor understanding of the role of vegetation in methane production, transport, and oxidation (Berrittella & van Huissteden, 2011; van Huissteden et al., 2009; Riley et al., 2011).

Vascular wetland plants are key factors in production, transportation, and oxidation of $CH_4$ (Joabsson et al., 1999; Laanbroek, 2010). Microbes produce $CH_4$ in the anaerobic subsurface of wetlands via methanogenesis, a process enhanced by sugars and amino acids released from plant roots, termed root exudates (Megonigal et al., 1999; Shannon & White, 1996; Ström et al., 2003; Whiting & Chanton, 1993). Emission occurs via three pathways: gas-bubble ebullition, diffusion through soil and/or water column, or diffusion through hollow aerenchyma tissue inside vascular vegetation, also known as plant-mediated transport. Frequently, the dominant pathway is plant-mediated transport (Laanbroek, 2010; Schimel, 1995; Van der Nat & Middelburg, 1998), which is thought to decrease oxidation by enabling methane to bypass oxic surface layers (Knoblauch et al., 2015; Marushchak et al., 2016; Sebacher et al., 1985; Watson et al., 1997). However, hollow aerenchyma tissues that facilitate $CH_4$ transport can also bring atmospheric oxygen belowground (Armstrong, 2000; Blossfeld et al., 2011; Frederiksen & Glud, 2006; Han et al., 2016), potentially oxidizing methane along the plant-transport pathway (Calhoun & King, 1997; Fritz et al., 2011; Gerard & Chanton, 1993; van der Nat & Middelburg, 1998).

Most empirical studies connect increased plant productivity with increased methane emissions (e.g., Kankaala et al., 2005; McEwing et al., 2015; Megonigal et al., 1999; Nielsen et al., 2017; Vann & Patrick Megonigal, 2003; Whiting & Chanton, 1993), and most large-scale wetland models couple $CH_4$ emissions to net primary productivity (Bridgham et al., 2013; Melton et al., 2013). However, some empirical studies found emissions to be minimally related to plant productivity, or even negatively correlated (e.g., Fritz et al., 2011; Neubauer et al., 2005; Sutton-Grier & Megonigal, 2011; Updegraff et al., 2001). These responses are attributed to plant-facilitated oxygenation of the subsurface inhibiting methanogenesis and increasing $CH_4$ oxidation. But plant-facilitated oxidation is poorly characterized, set as a constant percentage of plant-mediated emissions in most wetland methane models (Ringeval et al., 2011; Walter & Heimann, 2000; Wania et al., 2010; Zhuang et al., 2004), though not all (see Riley et al. (2011)). This fact reflects uncertainty in the extent to which different plant species oxygenate the rhizosphere and the ability of methanotrophs to compete with other heterotrophic microbes for oxygen (Calhoun & King, 1997; Riley et al., 2011; Segers et al., 2001; Whalen, 2005).

In this study, we disentangled the mechanisms by which vascular vegetation affect wetland methane emissions. At a thermokarst bog complex in Interior Alaska, we utilized field-deployed planar optical oxygen sensors, microbial DNA analysis, and vegetation manipulation treatments (natural vegetation, no vascular vegetation, and simulated aerenchyma treatments) to identify the: 1) importance of aerenchyma in transporting methane from soil to atmosphere, 2) ability of aerenchyma to transport oxygen belowground, 3) extent to which aerenchyma transport affects methane oxidation, and 4) non-physical or 'biological' influence (associated with root carbon exudation and/or root-associated microbial communities) of vegetation on methane

production and oxidation. *Carex aquatilis* was the species of interest, as it emits the majority of plant-mediated methane emissions at the site (SI Fig. S1).

## 2 Materials and Methods

### *2.1. Field Site*

Data were collected May to September 2015 in a collapse scar bog within the Bonanza Creek Long Term Ecological Research forest in Interior Alaska (64.70 ºN, -148.3 ºW). The bog is part of a thawing wetland complex located within a black spruce forest underlain by ice-rich permafrost. Thaw commenced at the site 50 to 400 years ago and is active along bog margins (Euskirchen et al., 2014; Klapstein et al., 2014). The centers of collapse scar bogs are where thaw initiated while edges represent areas that recently thawed. Bog edges include open water transitioning into *Sphagnum riparium* hummocks with vascular plants such as water sedge (*Carex* spp.), bog rosemary (*Andromeda polifolia* L.), cotton grass (*Eriophorum* spp.), and leather leaf (*Chamaedaphne calyculata*.). Older bog centers are dominated by *Sphagnum* spp. hummocks that support woody species such as dwarf and bog birch (*Betula nana* and *B. glandulosa*), and larch (*Larix laricina*) (Finger et al., 2016). Hollows in the bog center support a diversity of vascular species similar to those of bog edges. *In situ* microbial rates and methane emissions are greater at the bog edge than in the center (Klapstein et al., 2014; Neumann et al., 2016). Data from 2009 and 2010 indicated that plant-facilitated methane emissions were driven by *Carex* species, accounting for ~66% of plant-mediated emissions at both the edge (±9%) and center (±11%) (SI Fig. S1). In 2015, *Carex* density was 72 (edge) and 39 (center) plants $m^{-2}$, averaging 55.5 plants $m^{-2}$.

### *2.2. Collar Treatments*

Six flux collars (61-cm x 61-cm x 26-cm; width x length x height) were positioned in the bog, three near the edge (0.8 to 2.4 m from edge) and three in the center (5.3 to 5.9 m from edge). Collars at both locations were subjected to one of three experimental treatments: natural-vegetation, simulated-aerenchyma, or *Sphagnum*-only. Thus, there was treatment replication between the bog edge and center, but not within each location.

For natural-vegetation collars, no manipulations were done. For *Sphagnum*-only and simulated-aerenchyma treatments, vascular plants were hand-pulled (including belowground roots) from the collar and within 20-cm of the perimeter. Disturbance to the over-winter methane pool was eliminated by removing vegetation prior to seasonal frost thaw, and plant removal was done carefully to minimize disturbance to *Sphagnum*. However, the approach could have formed conduits through the peat (Verville et al., 1998), and/or left roots behind that provided carbon for methanogenesis, both of which would have caused an overestimation of methane emissions from non-vegetated treatments. Removed vegetation was categorized as forb, shrub or graminoid and weighed prior to manipulations (SI Table S1). Plants were weeded throughout the season.

The method of King et al. (1998) was adapted to create the simulated-aerenchyma treatment. After plant removal, gas permeable silicone tubing (Dow Corning™ Silastic™ Tubing, 1.47mm inner diameter, 0.23 mm wall thickness) was inserted into peat matching site density of *Carex* (225 tubes $m^{-2}$, equating to ~56 'plants' per $m^{-2}$ with a 'plant' represented by a bundle of four tubes). Tubes were tied at the bottom to keep water out and inserted to at least 30-

cm. Tubing above the peat was held upright with copper wire. Tubes mimicked aerenchyma by providing a diffusive pathway for subsurface gases to travel to the atmosphere. However, conductance along the tube pathway was likely greater than that of the plant pathway because stomata and root tissues provide resistance to gas flow (Kelker & Chanton, 1997; Morrissey et al., 1993; Schimel, 1995). In addition, tube conductance was constant, whereas plant conductance can change diurnally (i.e., with stomatal conductance) and/or over the season (i.e., with plant growth).

Depth of surface seasonal frost was measured throughout the season at the corners of every collar.

### *2.3. Methane Fluxes*

#### *2.3.1. Collar Fluxes*

Methane flux was measured from collars using the static-chamber method. For standard flux measurements, well-mixed gas from opaque flux chambers (61-cm cubes) was sampled every 5 minutes over a 30-minute period into 20 mL plastic syringes. Two non-standard chamber flux measurements were conducted. The first, termed an 'anaerobic' flux, estimated the fraction of methane oxidized along the emissions pathway. The method was adapted from van der Nat and Middelburg (1998). The second non-standard flux, termed a 'dark' flux, provided a check on the 'anaerobic' flux method, indicating if extended darkness during the anaerobic fluxes influenced methane emissions. Fluxes were done the same time each day from 11:00 to 14:00, matching with the period of peak emissions at the bog complex (SI Fig. S2).

The anaerobic flux was initiated with a standard flux, after which the chamber was left on the collar, connected to an 80 $ft^3$ nitrogen cylinder and flushed with nitrogen for ~15 minutes during which ⅓ of the gas tank was emptied. Chambers were kept anaerobic for 180 minutes by trickling another ⅓ of the tank into the chamber. Finally, the last ⅓ of the tank was emptied into the chamber over ~15 minutes. Immediately after the final nitrogen flush, gas samples were collected following the same method as the standard flux. The length of the nitrogen trickle was established after tests with an oxygen electrode indicated anaerobic conditions inside the chamber after ~180 minutes. This approach assumes that relative to the initial standard flux, additional methane is emitted after the nitrogen flush, representing methane that was oxidized during the standard flux but escaped oxidation during the anaerobic flux.

The dark flux measurement mimicked an anaerobic flux except for the nitrogen flush. Instead of the flush, chambers were placed askew on the collar, enabling oxygenation of the chamber while keeping treatments dark. This configuration was maintained for ~210 minutes, matching the full length of a nitrogen flush (initial flush, trickle and final flush). The chamber was then returned to the collar for gas sampling. A few dark fluxes were conducted in 2015, but most were conducted in 2016 to assess the influence of extended darkness on treatments. These fluxes do not determine the absolute effect of darkness, but assess if darkness differentially affected the emission of methane from vegetated and non-vegetated treatments (e.g., by causing stomata to close and/or stopping photosynthesis).

#### *2.3.2. Individual Plant Fluxes*

Standard and anaerobic fluxes were performed on individual *Carex* plants using a flux chamber constructed of a 1-m long, 10-cm diameter pipe (SI Fig. S3). A mechanical plastic plug (Oatey Company, Inc., Cleveland, OH) sealed the top, and a black rubber stopper sealed the bottom. The rubber stopper had a slit extending from the outer edge to a center hole into which the base of a plant was slid. The stopper was placed on the peat surface and gaps between the stopper and the plant were sealed with vacuum grease to facilitate a gas-tight connection with the chamber. Chambers were positioned over the chosen plant onto the rubber stopper and held in place with a clamp that extended from the boardwalk. The plug was then inserted to create a closed system containing the entire aboveground portion of the plant. Three to six representative plants extending from the bog edge to center were selected for each measurement event.

Standard plant-level methane fluxes (refer to section 2.3.1) were conducted by sampling gas into syringes every five minutes over a 20-min period. Anaerobic fluxes were conducted by flushing the system with three chamber volumes of nitrogen gas and then trickling with nitrogen gas for 60 minutes, after which the chambers were flushed again before collection of samples. This flushing-sampling procedure was repeated two more times. The maximum flux rate from the three anaerobic sampling events was used as the anaerobic flux value. This staggered approach allowed achievement of anaerobic conditions while minimizing time plants were in the dark; it was not possible to directly measure root-zone oxygen concentrations of an individual plant due to proximity of other roots.

### *2.3.3. Analysis and Processing of Flux Samples*

Gas flux samples were analyzed within 24-hours of collection using a gas chromatograph outfitted with a flame ionization detector and Haysep Q column (Varian Inc., Palo Alto, CA, USA). A three-point calibration was used: 0, 10, and 100 ppmv $CH_4$ (Air Liquide America Specialty Gases, Plumsteadville, PA). Standards (10 ppmv) were run every 20 samples. A linear regression of $CH_4$ concentration versus time was fit to determine flux rates (mg $CH_4$ $m^{-2}$ $day^{-1}$). Standard error of the fitted slope was used to characterize error. Fluxes containing ebullition events, identified manually by sporadic jumps in methane concentration, were excluded (4% overall data). Only data from fluxing events that resulted in successful flux measurements from all six collars were used.

For anaerobic fluxes, the fraction of methane oxidized ($CH4_{fracOxidEmit}$) was calculated as: $CH4_{fracOxidEmit} = \frac{CH4_{nitrogen} - CH4_{standard}}{CH4_{standard}}$, where $CH4_{nitrogen}$ is the flux measured after the nitrogen flush and $CH4_{standard}$ is the flux measured before the nitrogen flush. The additional methane released during $CH4_{nitrogen}$ relative to $CH4_{standard}$ was attributed to methane oxidized prior to the nitrogen flush that escaped oxidation after the flush. Dividing the flux difference ($CH4_{nitrogen} - CH4_{standard}$) by $CH4_{standard}$ normalizes oxidized methane to emitted methane, enabling comparisons across treatments. Normalization by the amount of produced methane can be calculated from $CH4_{fracOxidEmit}$ as: $CH4_{fracOxidProd} = \frac{CH4_{fracOxidEmit}}{1 + CH4_{fracOxidEmit}}$. Note that 'produced' methane only includes that which was produced and transported, not what remained in porewater. Data are presented both ways, as normalization to emitted methane facilitates comparison to emissions, which is often the only reported value, while normalization to produced methane indicates how much oxidation reduced potential emissions. Similarly, for dark control fluxes, the relative difference between dark and standard emissions ($CH4_{relDarkEmit}$) was calculated as:

$CH4_{relDarkEmit} = \frac{CH4_{dark} - CH4_{standard}}{CH4_{standard}}$, where $CH4_{dark}$ is the flux after the dark period and $CH4_{standard}$ is the flux before the dark period.

Cumulative methane emissions from each treatment were calculated by integrating daily measurements over the season (108 days) using the midpoint Riemann sum method. The seasonal fraction of methane oxidized was calculated by (1) multiplying daily emissions by the measured fraction of methane oxidized to get a daily amount of methane oxidized, (2) integrating these values over the season using the midpoint Riemann sum method to get the seasonal amount of methane oxidized, and (3) normalizing cumulative methane oxidation by cumulative methane emissions. Standard error propagation techniques were used at each step of the integration process.

Differences in emissions between treatments were calculated to parse out the effects of biological and physical-transport processes. These differences were determined for each flux event, and for cumulative seasonal values. The difference between simulated-aerenchyma and *Sphagnum*-only treatments was interpreted as the effect aerenchyma have on physical methane transport from soil into the atmosphere. The difference between natural-vegetation and simulated-aerenchyma treatments was interpreted as the non-physical or biological effect of plants on methane production. Standard error propagation techniques were used.

### *2.4. Planar Optical Oxygen Measurements (Optodes)*

Planar optical oxygen sensors (optodes) enable quantitative visualization of oxygen concentrations at high spatial resolution across a two-dimensional surface. We adopted and modified the technology of Larsen et al. (2015). See SI Fig. S4 for details about the optode technology. Two optode sensors were attached as windows (88.9-cm tall x 55.9-cm wide) on separate sides of a hollow box (94.0-cm tall x 55.9-cm long x 55.9-cm wide) built out of 2.54-cm thick extruded PVC sheets (SI Fig. S4a). Dye and graphite coatings on optodes faced outward. This setup enabled visualization of oxygen concentrations and placement of imaging equipment inside the box (SI Fig. S4b). At the bog, a hole between the edge and center locations was carefully dug such that adjacent vegetation was minimally impacted (SI Fig. S4c). The box was placed in the hole and optode windows were pushed against the peat. The box was anchored to deep mineral soil using fence posts and weighted down using steel bricks (SI Fig. S4d) to offset water displacement. When not in use, the open top of the box was covered with a water-proof cap. A black tent was placed over the box during imaging approximately three times per month.

After installation, vascular vegetation was removed from a ~30-cm strip adjacent to one optode face and continually weeded throughout the season. In addition, along the outer edge of this optode, two silicone tubes matching those used in the simulated-aerenchyma treatment were inserted. The other optode face was left unaltered with natural vegetation.

### *2.5. Oxygen Injection and Decay Experiments*

Oxygen injection and decay experiments were conducted using field optodes. Water was withdrawn from the bog into a syringe, oxygenated by bubbling in atmosphere, and injected into the bog against the optode face where decay of oxygen was tracked over time. Bog water was withdrawn ~15-cm from and injected directly against both optode faces (with and without

natural vegetation) at 15- and 38-cm below the surface. For the optode without vascular vegetation, water withdrawal occurred within the unvegetated buffer strip. Two stainless-steel sipper tubes with unidirectional screens were used along with a low-flow peristaltic pump to control location and speed of water withdrawals and injections.

Immediately prior to, during and after the oxygen injection, multiple optode images were taken. For each image, total oxygen present was calculated by summing oxygen present in each pixel, determined by multiplying measured oxygen concentrations within a pixel by the pixel area. These summed values were plotted against time for an injection series. Pre-injection values established baseline conditions and the maximum value was used to normalize the data. An example of a normalized injection and decay curve is shown in SI Fig. S5. Decay portions of curves were fit with a first-order decay equation. The fitted decay constant and associated confidence intervals were used to compare rates of oxygen consumption across different injection experiments.

### *2.6. Microbial Community Analysis*

Cores for microbial analyses were taken in July, August, and September 2015 from within 15m of the flux collars at three different randomized locations spanning between bog edge and center. Due to the destructive nature of coring, we were unable to take cores near treatment collars. These cores therefore represent natural, unmanipulated bog conditions. We used freeze coring in which a dry-ice and ethanol mixture was poured down a 1.5m hollow metal tube inserted into the ground, causing soil to freeze on the exterior of the tube. After ~10 minutes the tube was pulled from the bog and subsampled at depths of 0-10, 10-20, 20-40, and 60-70 cm, which were immediately placed on dry ice for shipment. DNA was extracted at Michigan Tech University as part of the Peatland Microbiome Intercomparison project and sequenced at the Joint Genome Institute (JGI). Ten grams of peat was pulverized using a BioSpec beadbeater (BioSpec Products, Bartlesville, OK) for 2 minutes. DNA was extracted from 0.5g of pulverized peat using a Powersoil DNA isolation kit (MoBio Laboratories Inc., Carlsbad, CA) and cleaned using MoBio PowerClean Pro cleanup kit. DNA was quantified using a Qubit Fluorometer. JGI sequenced the V4 region of 16S rRNA using primers 515F and 805R (10µM) using 10ng DNA/µl and QuantaBio 5PRIME HotMasterMix (VWR International, Visalia, CA) (Caporaso et al., 2011). Samples were sequenced on an Illumina MiSeq platform (Illumina Inc., San Diego, CA) using 2 x 300 bp chemistry. Amplicon libraries were analyzed using the iTagger v2.1 pipeline.

No significant effect of location on methane oxidizer or methanogen abundance was detected, so statistical analyses used samples from all locations as true replicates. An Analysis of Covariance (ANCOVA) was run with depth as a categorical variable and month as a covariate, using the normalized relative abundance of methane oxidizers or methanogens weighted by DNA concentration due to the large variation in DNA concentration with depth.

### *2.7. Study Trade-Offs*

The use of multiple approaches within this study came at the cost of replication for the plant manipulation treatments. The treatments were replicated within two locations of the bog (edge and center) known to have different plant community compositions and emit different

amounts of methane (Neumann et al., 2016, Finger et al., 2016, Neumann et al., 2019), but there was not replication of each treatment within each location. This tradeoff was dictated by time and human-resource limitations in a remote field site. Studying two different bog locations and using multiple approaches was prioritized as it enabled probing of the various biogeochemical processes within the methane cycle affected by vascular vegetation. Therefore, results from the collar fluxes can indicate differences between individual collars, but they cannot statistically verify if differences were due to the applied treatments. Nonetheless, results from the treatment collars provide useful insights about general patterns and trends of methane production, oxidation and emissions at the studied locations within the bog, particularly when paired with results from other methods used in the study.

## 3 Results

### *3.1. Methane Emissions from Treatment Collars*

For all treatment collars, methane emissions on a given day were, in general, greater at the bog edge than in the bog center (Fig. 1a-c). As such, cumulative seasonal methane emissions from collars at the bog edge were greater than those in the center for all treatments (Fig. 1d, Table 1). Within each location, cumulative methane emissions were greatest for natural-vegetation treatments, followed by simulated-aerenchyma treatments, and least for *Sphagnum*-only treatments (Fig. 1d, Table 1). Cumulative emissions from collars with natural vegetation were 3.6 ($\pm$0.4 standard error (SE), edge and $\pm$0.2 SE, center) g $m^{-2}$ $season^{-1}$ larger than cumulative emissions from collars with simulated aerenchyma, and 4.1 ($\pm$0.2 SE, center) to 5.2 ($\pm$0.2 SE, edge) g $m^{-2}$ $season^{-1}$ larger than cumulative emissions from collars with only *Sphagnum* (Table 1).

At both locations, emissions from natural-vegetation treatments continually increased over the season (Mann Kendall p-value < 0.01, Fig. 1a), with much of the increase visually occurring after thaw of seasonal frost in early July. There was no statistically significant seasonal trend for simulated-aerenchyma or *Sphagnum*-only treatments. Instead, emissions from simulated-aerenchyma treatments appeared to increase after frost thaw and decrease back to pre-thaw levels after one month (Fig. 1b), while emissions from *Sphagnum*-only treatments appeared consistent for the entire season (Fig. 1c).

Differences in daily flux measurements between treatments qualitatively indicate that the continual post-thaw increase in methane emissions from natural-vegetation treatments was facilitated by both biological and physical-transport processes (Fig. 2a). These differences indicate that "aerenchyma" transport, represented by the difference between simulated-aerenchyma and *Sphagnum*-only treatments, increased emissions only during the first month post-thaw (Fig. 2b). Meanwhile, non-physical or biological processes, represented by the difference between natural-vegetation and simulated-aerenchyma treatments, increased emissions later in the season (Fig. 2c).

### *3.2. Methane Oxidation in Treatment Collars*

For each treatment, methane oxidation was similar between collars at the bog edge and center (SI Fig. S6a). Combining edge and center data for a given treatment further showed that

the fraction oxidized by treatments without vascular vegetation (i.e., *Sphagnum*-only and simulated-aerenchyma treatments) were highly similar (SI Fig. S6b). As such, oxidation data were consolidated into two populations: treatments with and without vascular vegetation (Fig. 3).

For each sampling event, the fraction of methane oxidized by treatments with natural vegetation was less than that oxidized by treatments without vegetation. As such, on a seasonal timescale, the fraction of methane oxidized by natural-vegetation treatments was ~20% of that emitted (17% of that produced), while oxidation in non-vegetated treatments was 60% of that emitted (38% of that produced) (Table 1). The magnitude of this difference changed over the season (Fig. 3). Notably, the fraction oxidized by vegetated treatments decreased throughout the season (Mann Kendall p-value = 0.017) while no trend was detected for non-vegetated treatments. By season's end, natural-vegetation treatments exhibited little to no oxidation (Fig. 3), aligning with the period when differences between treatments qualitatively indicated that methane emissions were driven by plant-facilitated biological processes (Fig. 2c).

Results from dark control fluxes indicate that oxidation differences between vegetated and non-vegetated treatments cannot be attributed to the method, namely keeping treatments dark for an extended period. There was not a notable difference between the fraction of methane lost during a dark flux (i.e., normalized difference between standard and dark emissions) between vegetated and non-vegetated treatments, and no trend was detected over the season for either treatment category (SI Fig. S6c,d).

### *3.3. Methane Emissions and Oxidation by Individual Carex Plants*

The average amount of methane emitted by individual *Carex* plants was 0.53 mg $CH_4$ $plant^{-1}$ $day^{-1}$ (± 0.08 SE, Fig. 4a). Data from all *Carex* fluxes were compiled because no trends were detected as a function of time or location (SI Fig. S7). Methane oxidation by individual *Carex* plants was minimal with an average oxidation of 4% (± 2% SE) of that emitted (Fig. 4b).

To compare emissions from individual plants to collar treatments, results were translated to an area basis using *Carex* density at the site (55.5 plant $m^{-2}$, the average of edge and center locations) and scaled to account for methane emissions from other vascular species (SI Fig. S1). On an area basis, the average emissions rate from individual *Carex* plants was 29 (± 4 SE) mg $m^{-2}$ $day^{-1}$ (Fig. 4a), which equated to a cumulative seasonal flux of 3.2 (± 0.4 SE) g $m^{-2}$ $season^{-1}$ (Table 1). Because *Carex* are responsible for ~66% of plant-mediated methane emissions (SI Fig. S1) the total vegetation flux scales up to an average emissions rate of 44 (± 7 SE) mg $m^{-2}$ $day^{-1}$ (Fig. 4a) or an average cumulative value of 4.8 (± 0.8 SE) g $m^{-2}$ $season^{-1}$ (Table 1). This calculated cumulative vegetation flux of 4.8 g $m^{-2}$ $season^{-1}$ aligns with differences in cumulative emissions between vegetated and non-vegetated treatments of 5.2 (± 0.2 SE) (edge) and 4.1 (± 0.2 SE) (center) g $m^{-2}$ $season^{-1}$ (Table 1).

### *3.4. Planar Optical Oxygen Measurements*

Planar optical oxygen sensors detected no belowground oxygen in the presence of natural vegetation (Fig. 5b), but did detect oxygen around simulated aerenchyma (i.e., silicone tubes) in the absence of vascular vegetation (Fig. 5a).

### *3.5. Methane Mass Balance*

To elucidate subsurface production, oxidation, and transport along different emission pathways, a mass balance was calculated based on cumulative seasonal methane emissions and oxidation from treatments with and without vascular vegetation (Table 2, SI Fig. S8). Results from individual plant measurements (Table 1, Fig. 4) were used to partition methane flux between the plant and peat-transport pathways within natural-vegetation treatments (Table 2, SI Fig. S8b,d). This approach assumes that the difference in cumulative methane emissions between *Sphagnum*-only and natural-vegetation treatments at a given location was due only to the presence of vegetation (i.e., cumulative methane emissions would have been identical between the two collars before vegetation was removed), and that methane emission and oxidation measured on individual *Carex* plants was representative of all *Carex* plants at the site.

The mass balance indicates methane production in natural-vegetation treatments was 3.5 ($\pm$0.4 SE, edge) and 3.0 ($\pm$0.3 SE, center) g $m^{-2}$ $season^{-1}$ greater than in *Sphagnum*-only treatments (Table 2). At both locations, the plant-transport pathway carried this additional methane to the atmosphere, and, at the bog edge, it siphoned methane away from the peat-transport pathway (Table 2, SI Fig. S8). Vascular plants carried 51% (edge) and 40% (center) of emitted methane from natural-vegetation treatments (Table 2).

The greater amount of methane emitted from natural-vegetation treatments relative to *Sphagnum*-only treatments (5.2$\pm$0.2, edge, and 4.1$\pm$0.2, center, g $m^{-2}$ $season^{-1}$; Table 2) was more than that which could be attributed to differences in methane production (i.e., 3.5$\pm$0.4, edge, and 3.0$\pm$0.3, center, g $m^{-2}$ $season^{-1}$; see paragraph above and Table 2). This discrepancy was explained by decreased methane oxidation in the presence of vegetation. Minimal oxidation occurred along the plant-transport pathway and, according to the mass balance, oxidation was decreased along the peat-transport pathway in the presence of vegetation. Thirty-seven percent ($\pm$2% SE) of transported methane was oxidized along the peat-transport pathway at both bog locations without vascular vegetation while 27% ($\pm$6% SE, edge) and 20% ($\pm$4% SE, center) was oxidized along this pathway with vascular vegetation (Table 2, SI Fig. S8).

### *3.6. Oxygen Injection and Decay*

At 15-cm, oxygen consumption appeared faster with vascular vegetation than without (Fig. 6). The average first-order decay rate constant was 4.6 ($\pm$0.1 SE) $hr^{-1}$ with vegetation and 3.0 ($\pm$0.3 SE) $hr^{-1}$ without vegetation (ignoring the outlier, defined as a point that is greater than the 3$^{rd}$ quartile or less than the 1$^{st}$ quartile by more than 1.5 times the interquartile range). However, vascular vegetation had no effect on oxygen consumption at 38-cm (Fig. 6). Data from this depth were combined resulting in an average first-order decay rate constant of 1.9 ($\pm$0.1 SE) $hr^{-1}$.

### *3.7. Abundance of Methane Oxidizers and Methanogens*

The ANCOVA for the relative abundance of methane oxidizers showed a significant effect of the categorical variable depth ($p=0.0002$, followed by Tukey Kramer HSD test), as well as the covariate month ($p=0.03$), with no interaction between them (SI Fig. S9). Methane oxidizers were highest in the surface 10-cm and abundance decreased over the season. The

overall adjusted R-squared was 0.48. Methane oxidizers were both Type I gamma-proteobacteria (*Methylococcales*) and Type II alpha-proteobacteria (*Methylobaceriaceae* and *Methylocystaceae*), beta-proteobacteria *Methylophilales*, and *Verrucomicrobia* genus *Candidatus methlylacidiphilum*. The dominant population (reflected in 16S rRNA relative abundance) of methane oxidizers was *Methylococcales.*

A similarly organized ANCOVA for methanogens showed an interaction between depth and month ($p = 0.03$, SI Fig. S10). Methanogens were most abundant at 20-cm and 40-cm, followed by 70-cm, and lowest at 10-cm. The relative abundance of methanogens increased over the season at 40-cm and remained stable at all other depths. The overall adjusted R-squared was 0.78.

## 4 Discussion

### *4.1. Methane Emissions at Bog Edge Versus Bog Center*

Cumulative seasonal methane emissions were greater from treatment collars at the bog edge than from those in the center (Table 1); though due to lack of replication within each location we cannot statistically confirm that emissions were greater at the edge than at the center. However, the permafrost-free, but actively thawing edge of a collapse scar bog is a known hotspot for emissions at this site (Klapstein et al., 2014, Neumann et al., 2016, Neumann et al., 2019) and others (Klapstein et al., 2014; Liblik et al., 1997; Neumann et al., 2016; Prater et al., 2007). Increased emissions along bog edges are potentially caused by 1) proximity to thawing permafrost, which releases organic carbon and nutrients useful to microbial and plant activity (Abbott et al., 2014; Anthony et al., 2016; Keuper et al., 2012), 2) runoff from surrounding permafrost plateaus, which transports atmospheric thermal energy into the bog and rapidly warms soil (Neumann el at., 2019), 3) higher water tables, which promote anaerobic soil conditions that favor methanogenesis, reduce methane oxidation, and promote colonization by sedges (Liblik et al., 1997; Olefeldt et al., 2013), and/or 4) greater abundance of sedges, which facilitate methane transport and release sugars and organic acids into soil that fuel methanogenesis (Olefeldt et al., 2013; Prater et al., 2007). All four of these mechanisms are plausible at this site given previous site measurements (Finger et al., 2016, Neumann et al., 2019).

Our results imply that while vegetation affects methane emissions, it is not responsible for increased emissions at the bog edge relative to the center at our site. At the edge, all treatment collars emitted more cumulative seasonal methane than corresponding collars in the center (Table 1). Additionally, the difference in emissions between treatments with and without vascular vegetation throughout the season was qualitatively similar at both locations (Fig. 2a), signifying that effects of vegetation operated on top of location-specific factors (e.g., proximity to thawing permafrost, higher water tables, etc.) that controlled baseline emissions.

### *4.2. Dual Role of Vascular Vegetation on Methane Emissions*

Methane emissions from collars with vascular vegetation increased in the late season (i.e., after July; Fig. 1a), facilitating greater cumulative seasonal methane emissions relative to non-vegetated treatment collars at each location (Table 1, Fig 1d). While the lack of collar treatment replication means we cannot statistically conclude that vegetation was responsible for

these differences, the two approaches used to assess the effects of vegetation — removing plants (i.e., collar treatments) and isolating plants (i.e., individual plant fluxes) — found a similar methane contribution from vascular vegetation. Removing plants suggested that vascular vegetation increased cumulative methane emissions by 4.1-5.2 g $m^{-2}$ $season^{-1}$ (Table 1), while isolating plants suggested that vascular vegetation increased emissions by 4.8 g $m^{-2}$ $season^{-1}$, after scaling for plant density and relative contributions of different species (Table 1).

It is established that vascular vegetation increase wetland methane emissions (Davidson et al., 2016; King et al., 1998; Marushchak et al., 2016; McEwing et al., 2015; Noyce et al., 2014; Olefeldt et al., 2013; Whiting & Chanton, 1992). This increase is attributed to both aerenchyma-enhanced transport of methane and release of organic carbon into soil that fuels methanogenesis. Disentangling these two factors is important for predicting how plants will affect future emissions; aerenchyma development and root carbon release will respond differently to increasing atmospheric carbon dioxide levels, warmer temperatures and altered precipitation and soil moisture patterns (Armstrong, 1980; Cheng, 1999; Gregory et al., 1995; Leakey et al., 2009; Visser et al., 2000).

We adopted the approach of King et al. (1998), using silicone tubes to simulate the aerenchyma transport capacity of vascular vegetation without associated 'biological' influences of plants. Simulated aerenchyma qualitatively increased methane emissions relative to *Sphagnum*-only treatments for a brief period in July after seasonal frost thaw (Fig. 2b). The methane released was likely generated over winter and made available for transport with thawing frost. King et al. (1998) saw a decrease in emissions from late July onwards in their simulated-aerenchyma treatment, similarly to our study (Fig. 1b from early August onwards). Collectively, these results signify that physical aerenchyma transport is important when there is a store of belowground methane, but 'biological' influences of vascular vegetation are necessary for continued methane generation.

The 'biological' influence of vascular vegetation appeared to increase over time, aligning with seasonal growth of vegetation. Peak biomass occurred in late July and differences between treatments indicated that 'biological' influences started dominating in late July to early August and facilitated a continued increase in emissions until the season's end (early September) (Fig. 2c). Methane emitted later in the season was likely generated during the growing season through fermentation of plant-derived organic carbon and/or by plant-associated microbes.

Methane oxidation in vegetated treatments also decreased over time (Fig. 3), reaching zero during the period when emissions appeared to be dominated by 'biological' influences of vascular vegetation (Fig. 2c). These responses imply that the 'biological' influence dominated when plants were fully mature (i.e., had reached peak biomass), and plants increased methane emissions by simultaneously increasing production and decreasing oxidation. Mass balance calculations confirm this contention, showing that production increased and oxidation decreased in vegetated treatments relative to non-vegetated treatments (Table 2, SI Fig. S8).

### *4.3 Methane Oxidation*

Early in the season, the amount of methane oxidized was ~50–80% of that emitted (~30–45% of that produced) in all treatments (Fig. 3). Normalized to production, this oxidation aligns with other direct measurements using chamber inhibition methods (i.e., chemical inhibitors or

oxic versus anoxic fluxes): 13–38% in wet sedge tundra on Alaska's North Slope (Moosavi & Crill, 1998), 20–40% in a *Carex*-dominated fen in Alberta, Canada early in the season (Popp et al., 2000), 30–39% in a *Carex*-dominated marsh in NE China early in the season (Ding et al., 2004), 15–32% in a freshwater marsh in Maine when soils were submerged (Roslev & King, 1996).

However, methane oxidation decreased over time in vegetated treatments such that by mid-August, oxidation no longer occurred (Fig. 3). This decrease dropped the cumulative seasonal fraction of methane oxidized from 0.60 in non-vegetated treatments to 0.17–0.21 in vegetated treatments when normalizing by emitted methane (from 0.38 to 0.15–0.17 when normalizing by produced methane) (Table 1). Others have directly measured a similar seasonal decrease in methane oxidation (Ding et al., 2004; Lombardi et al., 1997; van der Nat & Middelburg, 1998; Popp et al., 2000). Results from our study indicate that the seasonal decrease in oxidation was related to plant growth; the fraction of methane oxidized was constant in non-vegetated treatments (Fig. 3).

Minimal methane oxidation occurred along the plant-transport pathway (Fig. 4b). It is often assumed that vascular vegetation oxygenate the subsurface, and studies have detected oxygen around wetland plant roots (Blossfeld et al., 2011; Frederiksen & Glud, 2006; Han et al., 2016). However, our optical oxygen sensors showed little to no oxygen around roots at the field site (Fig. 5), indicating that either plants were not transporting oxygen belowground, or rates of oxygen consumption matched or exceeded rates of oxygen delivery. This absence of rhizosphere oxygenation supports the lack of methane oxidation measured along the plant-transport pathway, as oxygen availability has been directly linked with root-associated methanotrophy (Calhoun & King, 1997).

Relative to *Sphagnum*-only treatments, simulated aerenchyma did not appear to increase the fraction of methane oxidized (Table 1, SI Fig. S6a,b), which is explained by the fact that the tubes increased oxic surface area across which methane diffusion and transport occurred. The optical oxygen sensors detected standing pools of oxygen around simulated aerenchyma (Fig. 5). Therefore, the tubes extended the peat-atmosphere interface deeper belowground, which simultaneously increased methane transport and oxidation, leaving normalized oxidation unchanged. This outcome reinforces the contention that reduced methane oxidation associated with vascular vegetation must have a 'biological' influence. Simulated aerenchyma alone facilitated transport of both methane and oxygen between the peat-atmosphere interface, and thus did not alter the fraction of methane oxidized.

### *4.4 Why Would Vascular Vegetation Decrease Methane Oxidation?*

Reduced methane oxidation in the presence of vascular vegetation is often attributed to transport of methane through aerenchyma tissues, allowing methane to bypass oxic surface layers where oxidation can occur (Knoblauch et al., 2015; Marushchak et al., 2016; Sebacher et al., 1985; Watson et al., 1997). As discussed in the previous section, this mechanism only decreases methane oxidation if oxygen transported belowground through aerenchyma is consumed by non-methanotrophic processes (e.g., root respiration and/or other heterotrophic microbes). In this study, measuring methane oxidation in treatments with and without vascular vegetation and in isolated plants enabled partitioning of methane transport and oxidation along plant- versus peat-emissions pathways (SI Fig. S8). Partitioning showed that reduced oxidation

associated with vascular vegetation was due in part to aerenchyma transport allowing methane to bypass oxic surface layers, but it was not fully explained by this mechanism. Vascular vegetation did siphon methane away from the peat-transport pathway (Table 2) and minimal methane oxidation occurred along the plant-transport pathway (Fig. 4b, SI Fig. S8), but vascular vegetation also decreased the fraction of methane oxidized along the peat-transport pathway.

The ability of vascular vegetation to reduce methane oxidation along the peat-transport pathway signifies that plants altered the soil environment and/or microbial community such that methane dynamics outside the rhizosphere were impacted. In agreement with flux data, the relative abundance of methane oxidizers in the bog surface, which was naturally vegetated, declined over the season, while the relative abundance of methanogens in deeper soils increased. Robroek et al. (2015) found that potential methane oxidation, as assessed by incubations of peat collected from treatments with and without vascular vegetation in a *Sphagnum*-dominated ombrotrophic peatland in Sweden, was highest in hummocks when both graminoids and ericoids were absent. The greater potential for methane oxidation in these incubations was associated with a shift in the microbial community (greater number of gene copies of type 1b methane oxidizing bacteria) and decrease in polysaccharide content of the peat. Robroek et al. (2015) theorized that the lack of carbon exuded from plant roots in the non-vegetated treatment caused substrate limitation for non-methanotrophic bacteria, enabling the methanotrophic bacteria to thrive.

Building upon this past work, we speculate that at our study site, decreased oxidation associated with vascular vegetation was caused by root exudates fueling an increase in other heterotrophic communities that outcompeted methanotrophs for available oxygen and other electron acceptors. This argument is supported by multiple lines of evidence from our study:

1. Minimal to no oxygen was detected around plant roots, but oxygen was detected around silicone tubes (Fig. 5). Assuming plants were transporting and releasing oxygen belowground, this finding implies that root exudates (not released by the silicone tubes) fueled microbial consumption of root-released oxygen.
2. Methane oxidation (Fig. 3) and relative abundance of methane oxidizers (SI Fig. S9) decreased over the season when plants were present. This decrease coincided with the time during which 'biological' influences of plants dominated physical influences, according to differences in methane emissions between the three treatments (Fig. 2). Plant release of carbon belowground is positively associated with productivity (Edwards et al., 2018; Farrar et al., 2003; Nielsen et al., 2017) and known to fuel growth of microbial communities (Robroek et al. 2015).
3. Oxygen consumption rates appeared to be fastest in shallow peat in the presence of vascular vegetation (Fig. 6). Rates appeared to be slower in shallow peat without vascular vegetation and in deeper peat where conceptually plant roots exert less of an influence. According to Michaelis-Menten kinetics, oxygen consumption is a function of the microbial community and substrate availability (Van Bodegom et al., 2001). The release of root exudates necessarily alters substrate availability, which in turn alters microbial community structure (Galand et al., 2005; Robroek et al., 2015). These results indicate plants facilitated competition among heterotrophic communities for available oxygen.

Literature often points to root carbon as a source for fueling methane production (Joabsson et al., 1999; Laanbroek, 2010). Here we have indirect evidence that these same exudates facilitate decreases in methane oxidation.

### *4.5 Modeling Implications*

Currently, models positively relate methane production with plant productivity, but methane oxidation has no direct connection with productivity. Our study points toward a seasonal increase in plant productivity and associated root exudates in fueling a decrease in methane oxidation (Fig. 3). This result, if validated at other sites, indicates that models should negatively correlate methane oxidation with plant productivity.

Many models assume 40–50% of methane traveling through plants is oxidized (Ringeval et al., 2011; Walter & Heimann, 2000; Wania et al., 2010; Zhuang et al., 2004). Riley et al. (2011), which has a more mechanistic representation of rhizospheric oxidation, estimated that globally, an average of ~60% of plant-transported methane is oxidized, with less oxidation occuring in northern than in southern lattitudes. Our measurements indicate that for *Carex*, plant-transported methane oxidation was minimal (~4% on average; Fig. 4b). Thus, in locations with high *Carex* density, 40-50% likely over estimates oxidation along the plant-transport pathway.

We found one other study that directly measured methane oxidation by *Carex*. Ström et al. (2005) used $^{14}C$ labelled acetate in a single field-obtained monolith to estimate that *Carex* oxidized 20-40% of root-zone methane. Our oxidation measurements conducted over a season on 20 undistrubed *Carex* plants had large variability and did reach as high as 51% (Figure 4b). This variability could explain the difference between our smaller average oxidation value and the larger estimate from Ström et al. (2005), which was based on one measurment.

### *4.6 Experimental Approach*

We used multiple methods to probe plant processes within a thermokarst bog, many of which were novel for a field campaign. The various lines of evidence facilitated a mechanistic interpretation that would not have been possible without the multi-pronged approach. However, this strategy came at the cost of treatment replication and therefore the ability to statistically confirm that treatment-collar results were due to the applied plant manipulations. Preferably, the study would have included either treatment replication within the two locations of the studied bog (edge and center), or replication of the entire experiment in nearby bogs. Ideally, future work can build upon the study approach with resources needed for experimental replication.

## 5 Conclusion

In the studied collapse scar bog, baseline methane emissions appeared to be driven by location-specific factors (e.g., proximity to thawing permafrost, higher water tables, etc.) rather than by vegetation, with greater cumulative methane emissions at the bog edge than center for all treatments (Fig. 1d). Effects of vascular vegetation operated on top of these location-specific factors. At both locations, cumulative methane emissions were greater in vegetated treatment collars than in non-vegetated treatment collars (Table 1, Fig. 1d), though this difference cannot be statistically attributed to vegetation due to a lack of treatment replication. However, the

estimated methane contribution from vegetation based on the treatment collars (4.1-5.2 g $m^{-2}$ $season^{-1}$) matched that estimated by isolating plants and measuring individual plant fluxes (4.8 g $m^{-2}$ $season^{-1}$, Table 1). Merging multiple lines of evidence in mass balance calculations suggest that methane production was greater and methane oxidation was smaller in the presence of vegetation (Table 2, SI Fig. S8). Minimal oxidation occurred along the plant-transport pathway (Fig. 4b) and oxidation was suppressed along the peat-transport pathway in the presence of vascular vegetation (Table 2, SI Fig. S8). These responses appeared biologically mediated and not due to methane transport through aerenchyma tissues (Figs. 2 & 3). We conjecture they were supported by plant root exudates. It is well established that root exudates fuel methanogenesis (Joabsson et al., 1999; Laanbroek, 2010). Our study points to a role for root exudates in fueling relative growth of non-methanotrophic microbial communities that outcompete methanotrophs for oxygen and other electron acceptors.

It is anticipated that plant productivity will increase with atmospheric concentrations of carbon dioxide and climate warming (Ainsworth & Long, 2004; Leakey et al., 2009). Root exudation of carbon is coupled with plant productivity (Edwards et al., 2018; Nielsen et al., 2017), implying that rates of exudation will increase in the future. Our study indicates that such an increase in exudation could facilitate greater methane emissions by both fueling methanogenesis and diminishing methanotrophy.

**Acknowledgements, Samples, and Data**

We thank Anna Tsai for field assistance and Jennifer Harden and David McGuire for participation in the APEX program. This material is based upon work supported by the U.S. Department of Energy, Office of Science, Office of Biological and Environmental Research (Award Number DE-SC- 0010338 to R.B.N.) and the USGS Land Change Science Program. Logistic support was provided by the Bonanza Creek LTER Program, which is jointly funded by NSF (DEB 1026415) and the USDA Forest Service, Pacific Northwest Research Station (PNW01-JV112619320-16). Microbial data came from the Joint Genome Institute (JGI Proposal 1445). We thank Erik Lilleskov and L. Jamie Lamit for leadership, lab work, and data management for the JGI project. This is contribution number 19-175-J of the Kansas Agricultural Experiment Station. Any use of trade names is for descriptive purposes only and does not imply endorsement by the U.S. Government. Data used in this publication are available on the Bonanza Creek LTER website (http://www.lter.uaf.edu/data/data-catalog).

## References


Abbott, B. W., Larouche, J. R., Jones, J. B., Bowden, W. B., & Balser, A. W. (2014). Elevated dissolved organic carbon biodegradability from thawing and collapsing permafrost: Permafrost carbon biodegradability. *Journal of Geophysical Research: Biogeosciences*, *119*(10), 2049–2063. https://doi.org/10.1002/2014JG002678

Ainsworth, E. A., & Long, S. P. (2004). What have we learned from 15 years of free-air CO2 enrichment (FACE)? A meta-analytic review of the responses of photosynthesis, canopy properties and plant production to rising CO2: Tansley review. *New Phytologist*, *165*(2), 351–372. https://doi.org/10.1111/j.1469-8137.2004.01224.x

Anthony, K. W., Daanen, R., Anthony, P., von Deimling, T. S., Ping, C.-L., Chanton, J. P., & Grosse, G. (2016). Methane emissions proportional to permafrost carbon thawed in Arctic lakes since the 1950s. *Nature Geoscience*, *9*(9), 679–682. https://doi.org/10.1038/ngeo2795

Armstrong, W. (1980). Aeration in Higher Plants. *Advances in Botanical Research*, *7*, 225–332. https://doi.org/10.1016/S0065-2296(08)60089-0

Armstrong, W. (2000). Oxygen Distribution in Wetland Plant Roots and Permeability Barriers to Gas-exchange with the Rhizosphere: a Microelectrode and Modelling Study with Phragmites australis. *Annals of Botany*, *86*(3), 687–703. https://doi.org/10.1006/anbo.2000.1236

Berrittella, C., & van Huissteden, J. (2011). Uncertainties in modelling $CH_4$ emissions from northern wetlands in glacial climates: the role of vegetation parameters. *Climate of the Past*, *7*(4), 1075–1087. https://doi.org/10.5194/cp-7-1075-2011

Blossfeld, S., Gansert, D., Thiele, B., Kuhn, A. J., & Lösch, R. (2011). The dynamics of oxygen concentration, pH value, and organic acids in the rhizosphere of Juncus spp. *Soil Biology and Biochemistry*, *43*(6), 1186–1197. https://doi.org/10.1016/j.soilbio.2011.02.007

Bridgham, S. D., Cadillo-Quiroz, H., Keller, J. K., & Zhuang, Q. (2013). Methane emissions from wetlands: biogeochemical, microbial, and modeling perspectives from local to global scales. *Global Change Biology*, *19*(5), 1325–1346. https://doi.org/10.1111/gcb.12131

Calhoun, A., & King, G. M. (1997). Regulation of root-associated methanotrophy by oxygen availability in the rhizosphere of two aquatic macrophytes. *Appl. Environ. Microbiol.*, *63*(8), 3051–3058.

Cheng, W. (1999). Rhizosphere feedbacks in elevated CO2. *Tree Physiology*, *19*(4–5), 313–320. https://doi.org/10.1093/treephys/19.4-5.313

Ciais, P., Sabine, C., Bala, G., Bopp, L., Brovkin, V., Canadell, J., et al. (2013). Carbon and other biogeochemical cycles. In *Climate change 2013: the physical science basis. Contribution of Working Group I to the Fifth Assessment Report of the Intergovernmental Panel on Climate Change* (pp. 465–570). Cambridge University Press.

Davidson, S. J., Sloan, V. L., Phoenix, G. K., Wagner, R., Fisher, J. P., Oechel, W. C., & Zona, D. (2016). Vegetation Type Dominates the Spatial Variability in CH4 Emissions Across Multiple Arctic Tundra Landscapes. *Ecosystems*, *19*(6), 1116–1132. https://doi.org/10.1007/s10021-016-9991-0

Denman, K. L., Brasseur, G., Chidthaisong, A., Ciais, P., Cox, P. M., Dickinson, R. E., et al. (2007). Couplings Between Changes in the Climate System and Biogeochemistry. In S. Solomon, D. Qin, M. Manning, Z. Chen, M. Marquis, K. B. Averyt, et al. (Eds.), *Climate Change 2007: The Physical Science Basis. Contribution of Working Group I to the Fourth Assessment Report of the Intergovernmental Panel on Climate Change* (p. 90). Cambridge, United Kingdom and New York, NY, USA: Cambridge University Press.

Ding, W., Cai, Z., & Tsuruta, H. (2004). Summertime variation of methane oxidation in the rhizosphere of a Carex dominated freshwater marsh. *Atmospheric Environment*, *38*(25), 4165–4173. https://doi.org/10.1016/j.atmosenv.2004.04.022

Edwards, K. R., Kaštovská, E., Borovec, J., Šantrůčková, H., & Picek, T. (2018). Species effects and seasonal trends on plant efflux quantity and quality in a spruce swamp forest. *Plant and Soil*, *426*(1), 179–196. https://doi.org/10.1007/s11104-018-3610-0

Etminan, M., Myhre, G., Highwood, E. J., & Shine, K. P. (2016). Radiative forcing of carbon dioxide, methane, and nitrous oxide: A significant revision of the methane radiative forcing. *Geophysical Research Letters*, *43*(24), 12,614-12,623. https://doi.org/10.1002/2016GL071930

Euskirchen, E. S., Edgar, C. W., Turetsky, M. R., Waldrop, M. P., & Harden, J. W. (2014). Differential response of carbon fluxes to climate in three peatland ecosystems that vary in the presence and stability of permafrost: Carbon fluxes and permafrost thaw. *Journal of Geophysical Research: Biogeosciences*, *119*(8), 1576–1595. https://doi.org/10.1002/2014JG002683

Farrar, J., Hawes, M., Jones, D., & Lindow, S. (2003). How Roots Control the Flux of Carbon to the Rhizosphere. *Ecology*, *84*(4), 827–837. https://doi.org/10.1890/0012-9658(2003)084[0827:HRCTFO]2.0.CO;2

Finger, R. A., Turetsky, M. R., Kielland, K., Ruess, R. W., Mack, M. C., & Euskirchen, E. S. (2016). Effects of permafrost thaw on nitrogen availability and plant-soil interactions in a boreal Alaskan lowland. *Journal of Ecology*, *104*(6), 1542–1554. https://doi.org/10.1111/1365-2745.12639

Frederiksen, M. S., & Glud, R. N. (2006). Oxygen dynamics in the rhizosphere of Zostera marina: A two-dimensional planar optode study. *Limnology and Oceanography*, *51*(2), 1072–1083. https://doi.org/10.4319/lo.2006.51.2.1072

Fritz, C., Pancotto, V. A., Elzenga, J. T. M., Visser, E. J. W., Grootjans, A. P., Pol, A., et al. (2011). Zero methane emission bogs: extreme rhizosphere oxygenation by cushion plants in Patagonia. *New Phytologist*, *190*(2), 398–408. https://doi.org/10.1111/j.1469-8137.2010.03604.x

Galand, P. E., Fritze, H., Conrad, R., & Yrjälä, K. (2005). Pathways for Methanogenesis and Diversity of Methanogenic Archaea in Three Boreal Peatland Ecosystems. *Applied and Environmental Microbiology*, *71*(4), 2195–2198. https://doi.org/10.1128/AEM.71.4.2195-2198.2005

Gerard, G., & Chanton, J. (1993). Quantification of methane oxidation in the rhizosphere of emergent aquatic macrophytes: defining upper limits. *Biogeochemistry*, *23*(2), 79–97. https://doi.org/10.1007/BF00000444

Gregory, P. J., Palta, J. A., & Batts, G. R. (1995). Root systems and root:mass ratio-carbon allocation under current and projected atmospheric conditions in arable crops. *Plant and Soil*, *187*(2), 221–228. https://doi.org/10.1007/BF00017089

Han, C., Ren, J., Tang, H., Xu, D., & Xie, X. (2016). Quantitative imaging of radial oxygen loss from Valisneria spiralis roots with a fluorescent planar optode. *Science of The Total Environment*, *569–570*, 1232–1240. https://doi.org/10.1016/j.scitotenv.2016.06.198

van Huissteden, J., Petrescu, A. M. R., Hendriks, D. M. D., & Rebel, K. T. (2009). Sensitivity analysis of a wetland methane emission model based on temperate and arctic wetland sites. *Biogeosciences*, *6*(12), 3035–3051. https://doi.org/10.5194/bg-6-3035-2009

Joabsson, A., Christensen, T. R., & Wallén, B. (1999). Vascular plant controls on methane emissions from northern peatforming wetlands. *Trends in Ecology & Evolution*, *14*(10), 385–388. https://doi.org/10.1016/S0169-5347(99)01649-3

Kankaala, P., Käki, T., Mäkelä, S., Ojala, A., Pajunen, H., & Arvola, L. (2005). Methane efflux in relation to plant biomass and sediment characteristics in stands of three common

emergent macrophytes in boreal mesoeutrophic lakes. *Global Change Biology*, *11*(1), 145–153. https://doi.org/10.1111/j.1365-2486.2004.00888.x

Keuper, F., van Bodegom, P. M., Dorrepaal, E., Weedon, J. T., van Hal, J., van Logtestijn, R. S. P., & Aerts, R. (2012). A frozen feast: thawing permafrost increases plant-available nitrogen in subarctic peatlands. *Global Change Biology*, *18*(6), 1998–2007. https://doi.org/10.1111/j.1365-2486.2012.02663.x

King, J. Y., Reeburgh, W. S., & Regli, S. K. (1998). Methane emission and transport by arctic sedges in Alaska: Results of a vegetation removal experiment. *Journal of Geophysical Research: Atmospheres*, *103*(D22), 29083–29092. https://doi.org/10.1029/98JD00052

Klapstein, S. J., Turetsky, M. R., McGuire, A. D., Harden, J. W., Czimczik, C. I., Xu, X., et al. (2014). Controls on methane released through ebullition in peatlands affected by permafrost degradation: Ebullition in peatlands with thermokarst. *Journal of Geophysical Research: Biogeosciences*, *119*(3), 418–431. https://doi.org/10.1002/2013JG002441

Knoblauch, C., Spott, O., Evgrafova, S., Kutzbach, L., & Pfeiffer, E.-M. (2015). Regulation of methane production, oxidation, and emission by vascular plants and bryophytes in ponds of the northeast Siberian polygonal tundra. *Journal of Geophysical Research: Biogeosciences*, *120*(12), 2015JG003053. https://doi.org/10.1002/2015JG003053

Laanbroek, H. J. (2010). Methane emission from natural wetlands: interplay between emergent macrophytes and soil microbial processes. A mini-review. *Annals of Botany*, *105*(1), 141–153. https://doi.org/10.1093/aob/mcp201

Larsen, M., Santner, J., Oburger, E., Wenzel, W. W., & Glud, R. N. (2015). O2 dynamics in the rhizosphere of young rice plants (Oryza sativa L.) as studied by planar optodes. *Plant and Soil*, *390*(1–2), 279–292. https://doi.org/10.1007/s11104-015-2382-z

Leakey, A. D. B., Ainsworth, E. A., Bernacchi, C. J., Rogers, A., Long, S. P., & Ort, D. R. (2009). Elevated CO2 effects on plant carbon, nitrogen, and water relations: six important lessons from FACE. *Journal of Experimental Botany*, *60*(10), 2859–2876. https://doi.org/10.1093/jxb/erp096

Liblik, L. K., Moore, T. R., Bubier, J. L., & Robinson, S. D. (1997). Methane emissions from wetlands in the zone of discontinuous permafrost: Fort Simpson, Northwest Territories, Canada. *Global Biogeochemical Cycles*, *11*(4), 485–494. https://doi.org/10.1029/97GB01935

Lombardi, J. E., Epp, M. A., & Chanton, J. P. (1997). Investigation of the methyl fluoride technique for determining rhizospheric methane oxidation. *Biogeochemistry*, *36*(2), 153–172. https://doi.org/10.1023/A:1005750201264

Marushchak, M. E., Friborg, T., Biasi, C., Herbst, M., Johansson, T., Kiepe, I., et al. (2016). Methane dynamics in the subarctic tundra: combining stable isotope analyses, plot- and ecosystem-scale flux measurements. *Biogeosciences*, *13*(2), 597–608. https://doi.org/10.5194/bg-13-597-2016

McEwing, K. R., Fisher, J. P., & Zona, D. (2015). Environmental and vegetation controls on the spatial variability of CH4 emission from wet-sedge and tussock tundra ecosystems in the Arctic. *Plant and Soil*, *388*(1), 37–52. https://doi.org/10.1007/s11104-014-2377-1

Megonigal, J. P., Whalen, S. C., Tissue, D. T., Bovard, B. D., Allen, A. S., & Albert, D. B. (1999). A Plant-Soil-Atmosphere Microcosm for Tracing Radiocarbon from Photosynthesis through Methanogenesis. *Soil Science Society of America Journal*, *63*(3), 665. https://doi.org/10.2136/sssaj1999.03615995006300030033x

Melton, J. R., Wania, R., Hodson, E. L., Poulter, B., Ringeval, B., Spahni, R., et al. (2013). Present state of global wetland extent and wetland methane modelling: conclusions from a model inter-comparison project (WETCHIMP). *Biogeosciences*, *10*(2), 753–788. https://doi.org/10.5194/bg-10-753-2013

Moosavi, S. C., & Crill, P. M. (1998). CH4 oxidation by tundra wetlands as measured by a selective inhibitor technique. *Journal of Geophysical Research: Atmospheres*, *103*(D22), 29093–29106. https://doi.org/10.1029/97JD03519

van der Nat, F.-J. W. A., & Middelburg, J. J. (1998). Seasonal variation in methane oxidation by the rhizosphere of Phragmites australis and Scirpus lacustris. *Aquatic Botany*, *61*(2), 95–110. https://doi.org/10.1016/S0304-3770(98)00072-2

Neubauer, S. C., Givler, K., Valentine, S., & Megonigal, J. P. (2005). Seasonal Patterns and Plant-Mediated Controls of Subsurface Wetland Biogeochemistry. *Ecology*, *86*(12), 3334–3344. https://doi.org/10.1890/04-1951

Neumann, R. B., Blazewicz, S. J., Conaway, C. H., Turetsky, M. R., & Waldrop, M. P. (2016). Modeling CH4 and CO2 cycling using porewater stable isotopes in a thermokarst bog in Interior Alaska: results from three conceptual reaction networks. *Biogeochemistry*, *127*(1), 57–87. https://doi.org/10.1007/s10533-015-0168-2

Nielsen, C. S., Michelsen, A., Strobel, B. W., Wulff, K., Banyasz, I., & Elberling, B. (2017). Correlations between substrate availability, dissolved CH4, and CH4 emissions in an arctic wetland subject to warming and plant removal. *Journal of Geophysical Research: Biogeosciences*, *122*(3), 645–660. https://doi.org/10.1002/2016JG003511

Noyce, G. L., Varner, R. K., Bubier, J. L., & Frolking, S. (2014). Effect of Carex rostrata on seasonal and interannual variability in peatland methane emissions. *Journal of Geophysical Research: Biogeosciences*, *119*(1), 24–34. https://doi.org/10.1002/2013JG002474

Olefeldt, D., Turetsky, M. R., Crill, P. M., & McGuire, A. D. (2013). Environmental and physical controls on northern terrestrial methane emissions across permafrost zones. *Global Change Biology*, *19*(2), 589–603. https://doi.org/10.1111/gcb.12071

Popp, T. J., Chanton, J. P., Whiting, G. J., & Grant, N. (2000). Evaluation of methane oxidation in therhizosphere of a Carex dominated fen in northcentral Alberta, Canada. *Biogeochemistry*, *51*(3), 259–281. https://doi.org/10.1023/A:1006452609284

Prater, J. L., Chanton, J. P., & Whiting, G. J. (2007). Variation in methane production pathways associated with permafrost decomposition in collapse scar bogs of Alberta, Canada. *Global Biogeochemical Cycles*, *21*(4), n/a-n/a. https://doi.org/10.1029/2006GB002866

Riley, W. J., Subin, Z. M., Lawrence, D. M., Swenson, S. C., Torn, M. S., Meng, L., et al. (2011). Barriers to predicting changes in global terrestrial methane fluxes: analyses using CLM4Me, a methane biogeochemistry model integrated in CESM. *Biogeosciences*, *8*(7), 1925–1953. https://doi.org/10.5194/bg-8-1925-2011

Ringeval, B., Friedlingstein, P., Koven, C., Ciais, P., Noblet-Ducoudré, N. de, Decharme, B., & Cadule, P. (2011). Climate-$CH_4$ feedback from wetlands and its interaction with the climate-$CO_2$ feedback. *Biogeosciences*, *8*(8), 2137–2157. https://doi.org/10.5194/bg-8-2137-2011

Robroek, B. J. M., Jassey, V. E. J., Kox, M. A. R., Berendsen, R. L., Mills, R. T. E., Cécillon, L., et al. (2015). Peatland vascular plant functional types affect methane dynamics by altering microbial community structure. *Journal of Ecology*, *103*(4), 925–934. https://doi.org/10.1111/1365-2745.12413

Roslev, P., & King, G. M. (1996). Regulation of methane oxidation in a freshwater wetland by water table changes and anoxia. *FEMS Microbiology Ecology*, *19*(2), 105–115. https://doi.org/10.1016/0168-6496(95)00084-4

Sebacher, D. I., Harriss, R. C., & Bartlett, K. B. (1985). Methane Emissions to the Atmosphere Through Aquatic Plants 1. *Journal of Environmental Quality*, *14*(1), 40–46. https://doi.org/10.2134/jeq1985.00472425001400010008x

Segers, R., Rappoldt, C., & Leffelaar, P. A. (2001). Modeling methane fluxes in wetlands with gas-transporting plants: 2. Soil layer scale. *Journal of Geophysical Research: Atmospheres*, *106*(D4), 3529–3540. https://doi.org/10.1029/2000JD900483

Shannon, R. D., & White, J. R. (1996). The effects of spatial and temporal variations in acetate and sulfate on methane cycling in two Michigan peatlands. *Limnology and Oceanography*, *41*(3), 435–443. https://doi.org/10.4319/lo.1996.41.3.0435

Ström, L., Ekberg, A., Mastepanov, M., & Røjle Christensen, T. (2003). The effect of vascular plants on carbon turnover and methane emissions from a tundra wetland. *Global Change Biology*, *9*(8), 1185–1192. https://doi.org/10.1046/j.1365-2486.2003.00655.x

Ström, L., Mastepanov, M., & Christensen, T. R. (2005). Species-specific Effects of Vascular Plants on Carbon Turnover and Methane Emissions from Wetlands. *Biogeochemistry*, *75*(1), 65–82. https://doi.org/10.1007/s10533-004-6124-1

Sutton-Grier, A. E., & Megonigal, J. P. (2011). Plant species traits regulate methane production in freshwater wetland soils. *Soil Biology and Biochemistry*, *43*(2), 413–420. https://doi.org/10.1016/j.soilbio.2010.11.009

Updegraff, K., Bridgham, S. D., Pastor, J., Weishampel, P., & Harth, C. (2001). Response of Co2 and Ch4 Emissions from Peatlands to Warming and Water Table Manipulation. *Ecological Applications*, *11*(2), 311–326. https://doi.org/10.1890/1051-0761(2001)011[0311:ROCACE]2.0.CO;2

Van Bodegom, P., Goudriaan, J., & Leffelaar, P. (2001). A mechanistic model on methane oxidation in a rice rhizosphere. *Biogeochemistry*, *55*(2), 145–177.

Vann, C. D., & Patrick Megonigal, J. (2003). Elevated CO2 and water depth regulation of methane emissions: Comparison of woody and non-woody wetland plant species. *Biogeochemistry*, *63*(2), 117–134. https://doi.org/10.1023/A:1023397032331

Visser, E. J. W., Colmer, T. D., Blom, C. W. P. M., & Voesenek, L. a. C. J. (2000). Changes in growth, porosity, and radial oxygen loss from adventitious roots of selected mono- and dicotyledonous wetland species with contrasting types of aerenchyma. *Plant, Cell & Environment*, *23*(11), 1237–1245. https://doi.org/10.1046/j.1365-3040.2000.00628.x

Walter, B. P., & Heimann, M. (2000). A process-based, climate-sensitive model to derive methane emissions from natural wetlands: Application to five wetland sites, sensitivity to model parameters, and climate. *Global Biogeochemical Cycles*, *14*(3), 745–765. https://doi.org/10.1029/1999GB001204

Wania, R., Ross, I., & Prentice, I. C. (2010). Implementation and evaluation of a new methane model within a dynamic global vegetation model: LPJ-WHyMe v1.3.1. *Geoscientific Model Development*, *3*(2), 565–584. https://doi.org/10.5194/gmd-3-565-2010

Watson, A., Stephen, K. D., Nedwell, D. B., & Arah, J. R. M. (1997). Oxidation of methane in peat: Kinetics of CH4 and O2 removal and the role of plant roots. *Soil Biology and Biochemistry*, *29*(8), 1257–1267. https://doi.org/10.1016/S0038-0717(97)00016-3

Whalen, S. c. (2005). Biogeochemistry of Methane Exchange between Natural Wetlands and the Atmosphere. *Environmental Engineering Science*, *22*(1), 73–94. https://doi.org/10.1089/ees.2005.22.73

Whiting, G. J., & Chanton, J. P. (1993). Primary production control of methane emission from wetlands. *Nature*, *364*(6440), 794–795. https://doi.org/10.1038/364794a0

Whiting, Gary J., & Chanton, J. P. (1992). Plant-dependent CH4 emission in a subarctic Canadian fen. *Global Biogeochemical Cycles*, *6*(3), 225–231. https://doi.org/10.1029/92GB00710

Zhang, Z., Zimmermann, N. E., Stenke, A., Li, X., Hodson, E. L., Zhu, G., et al. (2017). Emerging role of wetland methane emissions in driving 21st century climate change. *Proceedings of the National Academy of Sciences*, *114*(36), 9647–9652. https://doi.org/10.1073/pnas.1618765114

Zhuang, Q., Melillo, J. M., Kicklighter, D. W., Prinn, R. G., McGuire, A. D., Steudler, P. A., et al. (2004). Methane fluxes between terrestrial ecosystems and the atmosphere at northern high latitudes during the past century: A retrospective analysis with a process-based

biogeochemistry model. *Global Biogeochemical Cycles*, *18*(3). https://doi.org/10.1029/2004GB002239

**Figure 1.** Methane emissions from bog edge (blue) and center (red) from treatments **(a)** with natural vegetation, **(b)** without vascular vegetation but with simulated aerenchyma (i.e., silicone tubes), and **(c)** without vascular vegetation. Pictures of treatment types are in top left corners of plots. Error bars represent plus and minus standard error of the fitted emissions slope. **(d)** Integrated cumulative sum of emission time-series with shading showing propagated error from individual fluxes. Vertical dashed line indicates the period during which surface seasonal frost fully thawed.

**Figure 2**. Difference in methane emissions between treatments at the bog edge (blue) and center (red). Emission differences between **(a)** natural-vegetation and Sphagnum-only treatments, due conceptually to both physical and biological effects of vascular vegetation; **(b)** simulated-aerenchyma and *Sphagnum*-only treatments, due conceptually to only physical effects of vascular vegetation on the methane cycle (i.e., aerenchyma influence); and **(c)** natural-vegetation and simulated-aerenchyma treatments, due conceptually to only biological effects of vegetation. Grey and brown panels mark the periods when differences in panel (b) and panel (c), respectivley, qualitatively increased above a baseline level. Vertical dashed line indicates when surface seasonal frost fully thawed. Error bars represent propagated error from individual fluxes.

**Figure 3.** The fraction of methane oxidized at both the bog edge and center in collars with (black circles) and without (empty squares) natural vegetation, including treatments with and without simulated aerenchyma. Brown panel marks the period when emissions were conceptually controlled by the biological effects of vegetation (according to emission differences; Fig. 2c).

**Figure 4.** Box and whisker plots of methane emitted and oxidized by individual *Carex* plants. **(a)** Methane emissions on a per plant basis and translated to an area basis using average *Carex* density of 55.5 plant $m^{-2}$ (left hand y-axes) and scaled to account for methane emissions from other vascular species (SI Fig. S1) (right hand y-axis). **(b)** Methane oxidation by *Carex* normalized to produced and emitted methane. Horizontal line on box and whisker plots marks the median and diamond marks the mean. Box edges mark the 25th and 75th percentiles. Whiskers denote extreme data points not considered outliers (marked with 'x' symbol).

**Figure 5.** Dissolved oxygen concentrations measured with two-dimensional optical oxygen sensors (optodes) installed at the field site (SI Fig. S4). Silicone tubes were placed at the far edge of the non-vegetated optode.

**Figure 6.** Fitted first-order rate constant from oxygen injection experiments (SI Fig. S5) conducted against vegetated and non-vegetated optode faces after thaw of seasonal frost. Rate constants from 15-cm depth with (black circles) and without (open circles) natural vegetation, and from 38-cm depth regardless of vegetation (grey squares). Consumption rate was anomalously high for the first shallow-depth injection conducted without vascular vegetation.

Figure 1

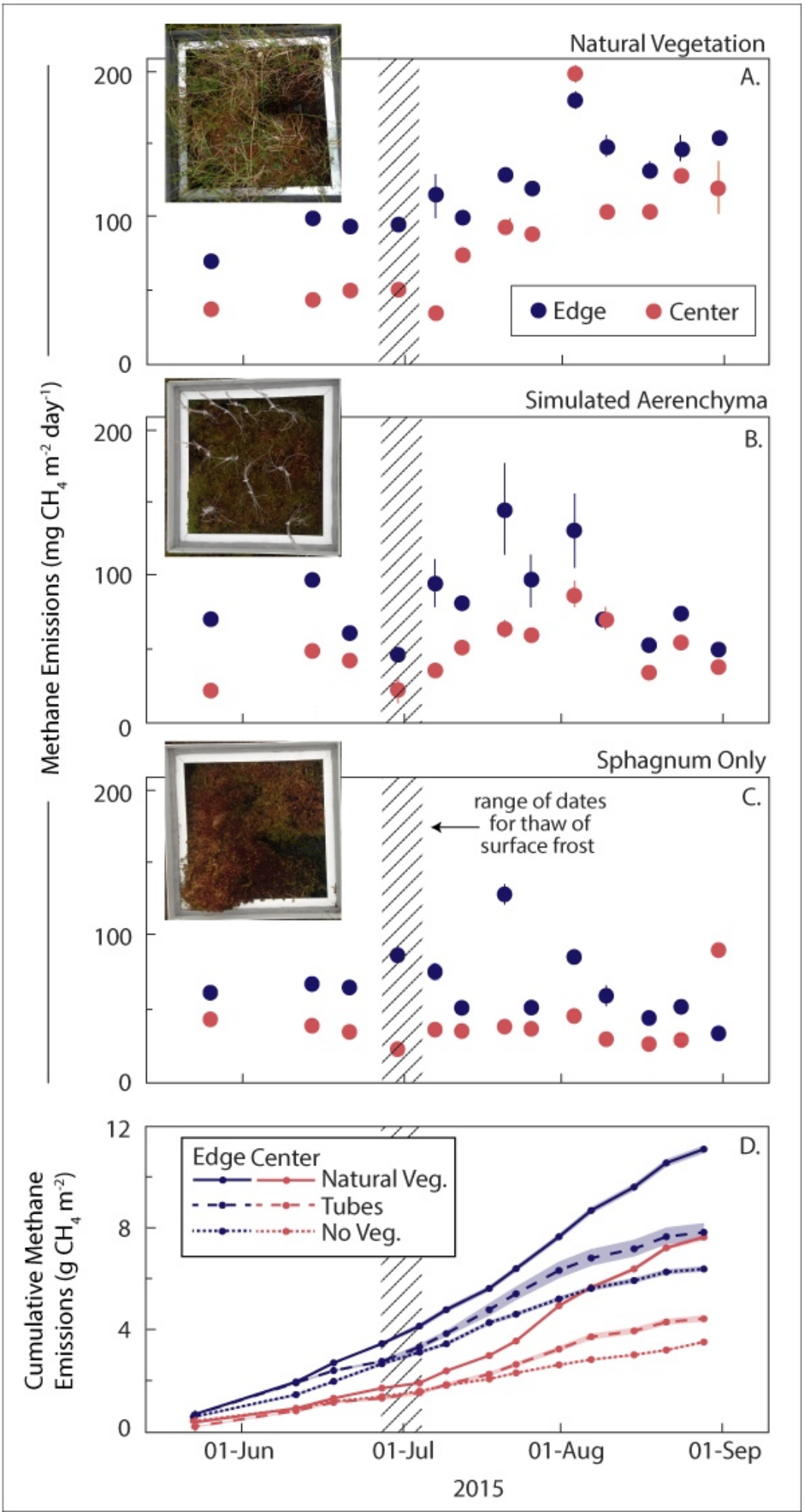
Natural Vegetation
A.
Simulated Aerenchyma
B.
Sphagnum Only
C.
range of dates for thaw of surface frost
Edge
Center
Methane Emissions (mg CH4 m-2 day-1)
200
100
0
D.
Edge Center
Natural Veg.
Tubes
No Veg.
Cumulative Methane Emissions (g CH4 m-2)
12
8
4
0
01-Jun
01-Jul
01-Aug
01-Sep
2015

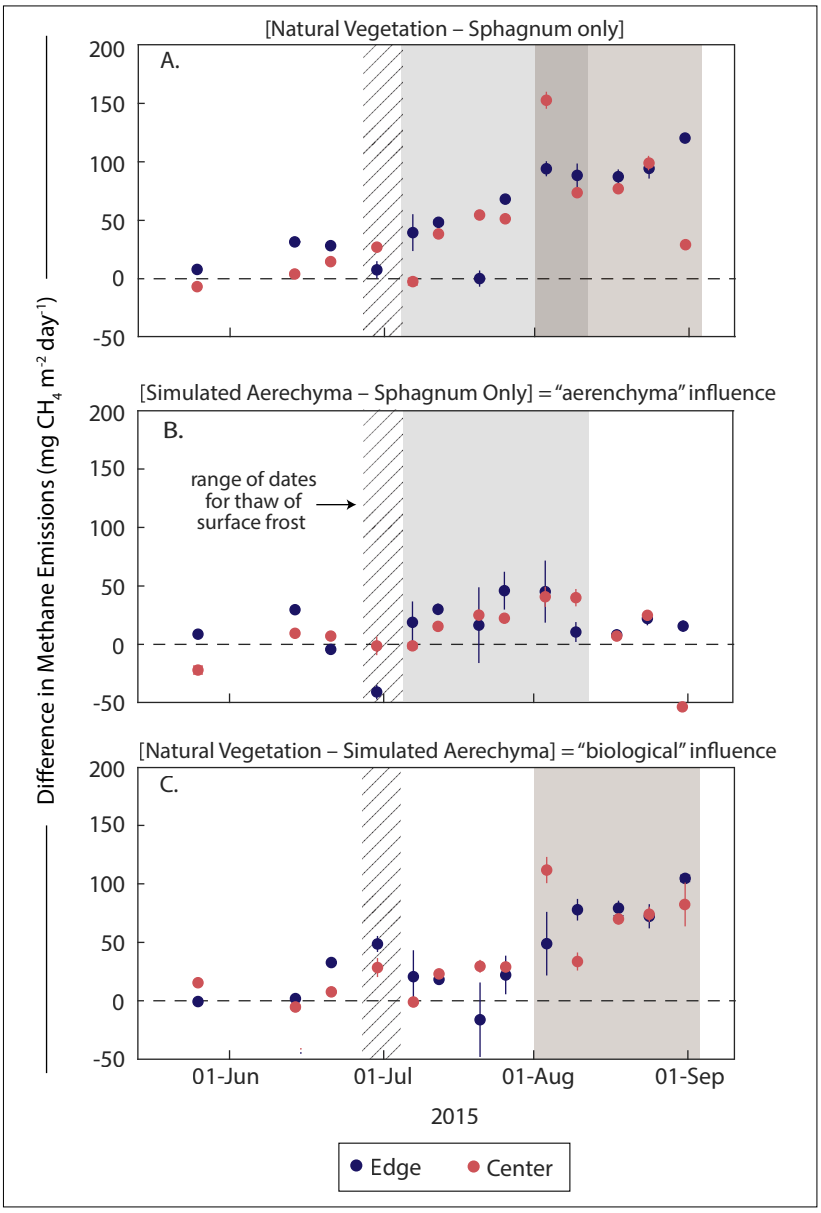
[Natural Vegetation – Sphagnum only]
A.
200
150
100
50
0
-50
[Simulated Aerechyma – Sphagnum Only] = "aerenchyma" influence
B.
range of dates
for thaw of
surface frost
[Natural Vegetation – Simulated Aerechyma] = "biological" influence
C.
Difference in Methane Emissions (mg CH4 m-2 day-1)
01-Jun
01-Jul
01-Aug
01-Sep
2015
Edge
Center

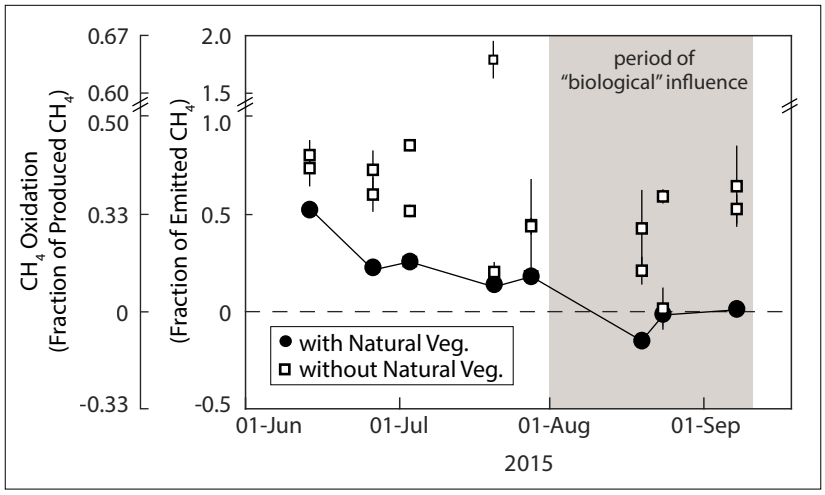
0.67
0.60
0.50
0.33
0
-0.33
CH4 Oxidation
(Fraction of Produced CH4)
2.0
1.5
1.0
0.5
0
-0.5
(Fraction of Emitted CH4)
period of
"biological" influence
with Natural Veg.
without Natural Veg.
01-Jun
01-Jul
01-Aug
01-Sep
2015

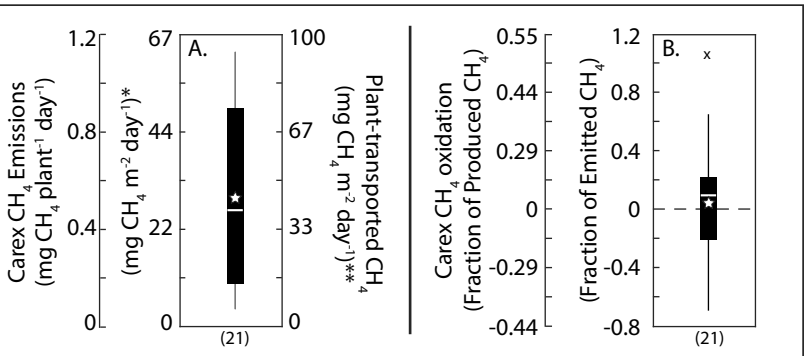


* assuming 55.5 Carex plants per $m^2$
** assuming Carex responsible for 66% of plant-mediated transport (SI Fig. S1)
☆ average Carex value

Field Optode Section — June 25-29, 2015

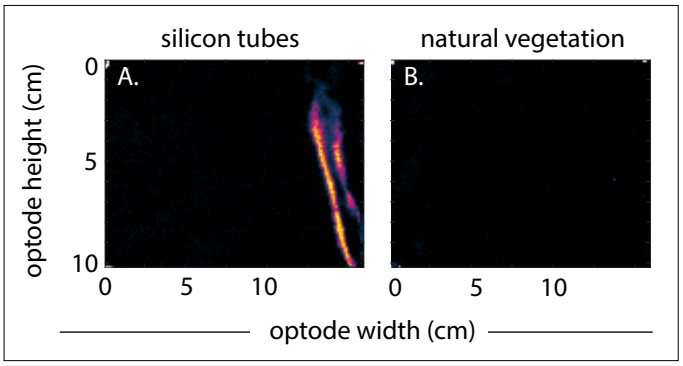


Legend

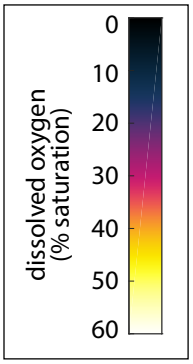

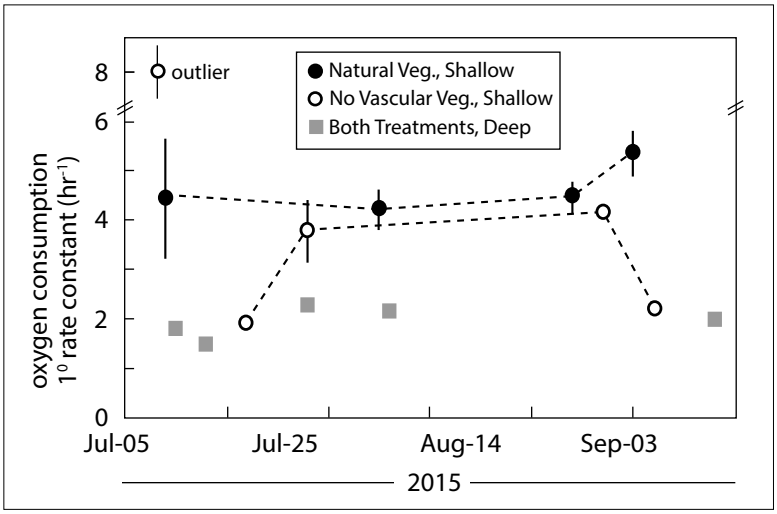
outlier
Natural Veg., Shallow
No Vascular Veg., Shallow
Both Treatments, Deep
oxygen consumption
1⁰ rate constant (hr⁻¹)
8
6
4
2
0
Jul-05
Jul-25
Aug-14
Sep-03
2015

**Table 1**

*Seasonal Cumulative Methane Emissions and Oxidation*

| Cumulative Values (± standard error) | $CH_4$ Emitted (g $m^{-2}$ $season^{-1}$) | $CH_4$ Oxidation (seasonal fraction of emitted $CH_4$) | $CH_4$ Produced (g $m^{-2}$ $season^{-1}$)* |
|---|---|---|---|
| **Natural Vegetation** | | | |
| Edge | 12.3 (±0.1) | 0.21[a] (±0.02) | 14.9 (±0.3) |
| Center | 8.4 (±0.2) | 0.17[a] (±0.03) | 9.8 (±0.3) |
| **Tubes w/out Vascular Vegetation** | | | |
| Edge | 8.7 (±0.3) | 0.60[b] (±0.04) | 13.9 (±0.5) |
| Center | 4.8 (±0.1) | | 7.6 (±0.2) |
| **No Vascular Vegetation** | | | |
| Edge | 7.1 (±0.1) | 0.60[b] (±0.03) | 11.4 (±0.3) |
| Center | 4.3 (±0.1) | | 6.8 (±0.2) |
| **Difference in Treatments at Edge** | | | |
| [Natural Veg.] – [Tubes] | 3.6 (±0.4) | -0.38 (±0.05) | 1.0 (±0.6) |
| [Natural Veg.] – [No Veg.] | 5.2 (±0.2) | -0.38 (±0.04) | 3.5 (±0.4) |
| [Tubes] – [No Veg.] | 1.5 (±0.3) | 0 (±0.05) | 2.5 (±0.6) |
| **Difference in Treatments at Center** | | | |
| [Natural Veg.] – [Tubes] | 3.6 (±0.2) | -0.43 (±0.04) | 2.2 (±0.3) |
| [Natural Veg.] – [No Veg.] | 4.1 (±0.2) | -0.43 (±0.04) | 3.0 (±0.3) |
| [Tubes] – [No Veg.] | 0.5 (±0.1) | 0 (±0.05) | 0.8 (±0.3) |
| **Individual *Carex* Plants** | | | |
| Edge | 4.1[c] (±0.6) | 0.08 (±0.04) | 4.4 (±0.6) |
| Center | 2.2[d] (±0.3) | | 2.4 (±0.3) |
| Site Average | 3.2[e] (±0.4) | | 3.4 (±0.4) |
| **Vascular Vegetation (Scaled from *Carex* Plants)[f]** | | | |
| Edge | 6.2 (±1.3) | 0.08 (±0.04) | 6.7 (±1.4) |
| Center | 3.4 (±0.7) | | 3.6 (±0.7) |
| Site Average | 4.8 (±0.8) | | 5.2 (±0.8) |

***** Calculated as (column 2)*(1+column 3).

[a] Measurements of the fraction of methane oxidized in edge and center collars with natural vegetation combined into one group and fit with a linearly decreasing trend line for seasonal calculation.

[b] Measurements of the fraction of methane oxidized in all collars without vascular vegetation treated as a group. Average value used in seasonal calculation.

[c-e] Calculated using average emissions rate for individual plants (Fig. 4) and [c]density of *Carex* plants at edge (26 plants in collar with area of 0.36 $m^2$ = 72 plants $m^{-2}$), [d]density of *Carex* plants in center (14 plants in collar with area of 0.36 $m^2$ = 39 plants $m^{-2}$), and [e]average density of *Carex* plants at site (average of edge and center locations = 55.5 plants $m^{-2}$).

[f] Scaling accounts for fact that *Carex* contribute to 66% of plant-mediated methane flux at the site (SI Fig. S1).

**Table 2**

*Results from Mass Balance Calculations*

| $CH_4$ g $m^{-2}$ $season^{-1}$ (±standard error) | Edge | | | Center | | |
|---|---|---|---|---|---|---|
| | Yes veg. [a] | No veg. [b] | Diff. [yes – no] | Yes veg. [a] | No veg. [b] | Diff. [yes – no] |
| **Production, Total** | 14.9 (±0.3) | 11.4 (±0.3) | +3.5 (±0.4) | 9.8 (±0.3) | 6.8 (±0.2) | +3.0 (±0.3) |
| Peat Pathway | 8.4 (±1.4) | 11.4 (±0.3) | -3.0 (±1.4) | 6.3 (±0.8) | 6.8 (±0.2) | -0.5 (±0.8) |
| % total | 56% (±9%) | 100% | n/a | 64% (±8%) | 100% | n/a |
| Veg. Pathway | +6.5 (±1.3) | n/a | +6.5 (±1.3) | 3.5 (±0.7) | n/a | +3.5 (±0.7) |
| % total | 44% (±9%) | n/a | n/a | 36% (±7%) | n/a | n/a |
| **Oxidation, Total** | **2.6 (±0.3)** | **4.3 (±0.2)** | -1.6 (±0.4) | **1.4 (±0.2)** | **2.6 (±0.1)** | -1.1 (±0.3) |
| Peat Pathway | 2.3 (±0.3) | **4.3 (±0.2)** | -2.0 (±0.4) | 1.3 (±0.2) | **2.6 (±0.1)** | -1.3 (±0.3) |
| % total | 87% (±16%) | 100% | n/a | 87% (±21%) | 100% | n/a |
| Veg. Pathway [c] | **0.3 (±0.2)** | n/a | +0.3 (±0.2) | **0.2 (±0.1)** | n/a | +0.2 (±0.1) |
| % total | 13% (±6%) | n/a | n/a | 13% (±6%) | n/a | n/a |
| **Oxidation, fraction of $CH_4$ produced** | 0.18 (±0.02) | 0.37 (±0.02) | -0.20 (±0.03) | 0.15 (±0.02) | 0.37 (±0.02) | -0.23 (±0.03) |
| Peat Pathway | 0.27 (±0.06) | 0.37 (±0.02) | -0.10 (±0.07) | 0.20 (±0.04) | 0.37 (±0.02) | -0.17 (±0.05) |
| Veg. Pathway | 0.05 (±0.03) | n/a | +0.05 (±0.03) | 0.05 (±0.03) | n/a | +0.05 (±0.03) |
| **Emissions, Total** | **12.3 (±0.1)** | **7.1 (±0.1)** | +5.2 (±0.2) | **8.4 (±0.2)** | **4.3 (±0.1)** | +4.1 (±0.2) |
| Peat Pathway | 6.1 (±1.3) | **7.1 (±0.1)** | -1.0 (±1.3) | 5.0 (±0.7) | **4.3 (±0.1)** | -0.8 (±0.7) |
| % total | 49% (±11%) | 100% | n/a | 60% (±9%) | 100% | n/a |
| Veg. Pathway [d] | **6.2 (±1.3)** | n/a | +6.2 (±1.3) | **3.4 (±0.7)** | n/a | +3.4 (±0.7) |
| % total | 51% (±11%) | n/a | n/a | 40% (±9%) | n/a | n/a |

**Red bold text** represents values that were measured; other values were calculated.

[a] Natural-vegetation treatments.

[b] *Sphagnum*-only treatments.

[c] Assuming no oxidation occurs through the plant-transport pathway for non-*Carex* vegetation.

[d] Scaled value from Table 1 that accounts for fact that *Carex* contribute to 66% of plant-mediated methane flux at the site (SI Fig. S1).